Check for updates

Received: 17 August 2022 | Accepted: 21 August 2022

DOI: 10.1002/mmce.23379

ORIGINAL ARTICLE

INTERNATIONAL JOURNAL OF RF AND MICROWAVE COMPUTER-AIDED ENGINEERING

WILEY

Design of GaN-based X-band LNAs to achieve sub-1.2 dB noise figure

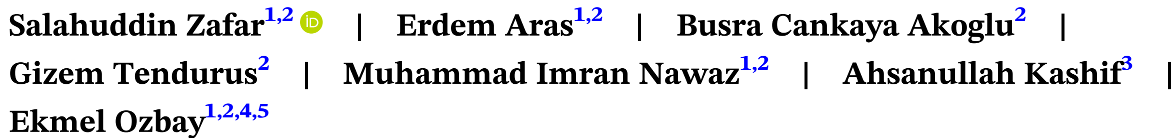

Salahuddin Zafar[1,2] | Erdem Aras[1,2] | Busra Cankaya Akoglu[2] | Gizem Tendurus[2] | Muhammad Imran Nawaz[1,2] | Ahsanullah Kashif[3] | Ekmel Ozbay[1,2,4,5]

[1]Department of Electrical and Electronics Engineering, Bilkent University, Ankara, Turkey

[2]Nanotechnology Research Center (NANOTAM), Bilkent University, Ankara, Turkey

[3]Department of Electrical Engineering, IIUI, Islamabad, Pakistan

[4]Department of Physics, Bilkent University, Ankara, Turkey

[5]UNAM Institute of Materials Science and Nanotechnology, Bilkent University, Ankara, Turkey

Correspondence

Salahuddin Zafar, Department of Electrical and Electronics Engineering, Bilkent University, Ankara, Turkey.

Email: salahuddin.zafar@bilkent.edu.tr

Funding information

Türkiye Bilimler Akademisi

Abstract

GaAs and SiGe technologies take an edge over GaN-based devices in terms of better noise figure (NF). In this article, we present HEMT topologies and design techniques to achieve a sub-1.2 dB NF for a GaN-based X-band low-noise amplifier (LNA). This NF is comparable with state-of-the-art reported works in competitive GaAs and SiGe technologies. Moreover, this is the best reported NF in X-band using GaN technology to date. Two LNAs are fabricated using in-house 0.15 μm AlGaN/GaN on the SiC HEMT process. LNA-1 has inductive source degenerated (ISD) HEMTs at both stages, while LNA-2 has ISD HEMT at the first and common source at the second stage. The significance of ISD HEMT, for the first or subsequent stages in a multi-stage design, towards NF improvement is addressed. The criticality of stability networks towards NF contribution and its design is discussed in detail. Furthermore, even-mode stability of each HEMT after complete LNA design is assured using the S-probe method in Pathwave Advanced Design Systems.

KEYWORDS

even-mode stability, GaN-on-SiC, inductive source degeneration, low-noise amplifier

1 | INTRODUCTION

Gallium nitride (GaN) technology combined with high electron mobility transistor (HEMT) emerged as the most suitable candidate for power applications at high frequencies. Over the years, GaN technology also started to take its place in low noise applications due to built-in power handling capability at the receive end, compact transceiver designs, and high linearity. On the other hand, gallium arsenide (GaAs) technology takes an edge regarding noise performance.[1,2,3,4,5] There are recently reported works[6,7,8,9] with promising NF for other competitive technologies, that is, SiGe BiCMOS and CMOS. A comparative noise investigation from DC –60 GHz, using 70 nm GaAs, and 60 nm GaN-on-Si processes, has shown superior noise performance of the GaAs process for most of the frequency range.[10]

Various approaches have been adopted to improve the noise characteristics for LNA design at the transistor and circuit levels. Vignesh et al.[6] have proposed quasi circulator LNA with the current reused technique to achieve optimized NF of less than 1.4 dB in X-band using 0.065 μm CMOS technology. Colangeli et al.[11] proposed three-stage LNA using 0.25 μm GaN-on-SiC technology by exploiting the same current-reuse architecture. The impedance between the base–collector terminals of common-emitter HBT is considered by Çalışkan et al.[7] to achieve sub-1 dB NF. Davulcu et al.[8] presented the first triple inductively degenerated cascode SiGe HBT in X-band. Kumar and Rebeiz[9] have proposed X- and K-

 © 2022 Wiley Periodicals LLC.

1099047x, 2022, 11, Downloaded from https://onlinelibrary.wiley.com/doi/10.1002/mmce.23379 by Bilkent University, Wiley Online Library on [22/02/2023]. See the Terms and Conditions (https://onlinelibrary.wiley.com/terms-and-conditions) on Wiley Online Library for rules of use; OA articles are governed by the applicable Creative Commons License

TABLE 1 A comparison of designed MMIC with the recently reported competitive technologies at X-band

Ref.	Freq. (GHz)	NF (dB)	IRC (dB)	ORC (dB)	Gain (dB)	Lg (μm)	Technology
Çalışkan et al.[7]	8–12	<1	<−9	<−24	>10	0.13	SiGe
Davulcu et al.[8]	8–12	<1.6[b]	<−10[b]	<−10[b]	>18	0.13	SiGe
Kanar et al.[9]	6.4–11	<1.3[b]	<−6[b]	<−2[b]	>21	0.18	SiGe
Zuo and Sun[29a]	8–12	<2.5	<−10	<−10	>30	0.25/0.45	GaAs
Xie et al.[30]	8–10	<1.4	<−8	<−8	>25	0.15	GaAs
Wang et al.[31]	10.7–13.1	<1.7[b]	<−8[b]	<−8[b]	>17[b]	0.15	GaAs
Zhou et al.[32]	8–12	<1.8	<−15[b]	–	>24	–	GaAs
Vignesh et al.[6]	8–12	<1.4	<−10[b]	<−10[b]	>25[b]	0.065	CMOS
Cao et al.[12]	8–12	<3.6	<−9[b]	<−16[b]	>13	0.13	CMOS
Ma et al.[33]	7.4–11.4	<3.8	<−12	<−8[b]	>23.5	–	CMOS
This work (LNA-1)	8–11	<1.2	<−10.3	<−10.1	>16.8	0.15	GaN

[a]Simulation-based.
[b]Estimated values from figures.

band LNAs with a method of noise match optimization with respect to the base inductor in a 0.18 μm SiGe HBT technology. Cao et al.[12] have proposed a pole converging technique to improve the noise figure (NF) over a broad range from 8 to 12 GHz using 0.13 μm CMOS technology. Zailer et al.[13] have demonstrated a method based on transistor size selection, that is, Cgs and simultaneous bias, to minimize the difference between NF and NF_{min} using 0.13 μm CMOS inductive source degenerated (ISD) cascode LNA. Sabzi et al.[14] have used a parallel design technique using 0.1 μm GaAs pHEMT technology to improve linearity and NF. Along with enhancing gain and linearity, they have achieved a low NF by optimizing the base inductor and placing an additional inductor between the second and third stages. Dai[15] proposed a novel modified complementary current-reused LNA using a forward body bias technique based on 0.18 μm RFSOI CMOS technology. Noise performance is improved by minimizing the body leakage by employing a diode-connected MOSFET forward bias. Sabzi et al.[16] demonstrated the reduction in overall NF in multistage LNAs by optimization of the first stage along with improvement in gain and input matching.

Improving the NF for GaN-based LNAs and making it close to GaAs has always been challenging. Various efforts have been made to improve and address the performance parameters of GaN-based LNAs, including linearity, robustness, recovery time, and NF.[2] Although sub-1.5 dB NF has been reported[4,17,18,19,20] for K- and Ka-bands, GaAs comparative NF at X-band for GaN technology remained a challenge. Yağbasan and Aktuğ[21] reported 1.6 dB NF using 0.25 μm GaN-on-SiC technology for 8–11 GHz. Recently,[22] sub-1.5 dB NF is reported in X-band using 0.09 μm GaN-on-SiC technology.

In this work, we designed 2-stage X-band LNAs with two different topologies based on 0.15 μm GaN-on-SiC technology. LNA-1 comprises inductively source degenerated (ISD) HEMTs at both stages, while LNA-2 is designed using ISD HEMT for the first stage only. ISD topology is used in LNA design to achieve a simultaneous match condition for source and optimum noise impedance, ensuring minimum NF and maximum gain.[23,24,25,26,27,28] In this study, a measurement model of common source (CS) HEMT is used to determine the value of the source degenerated (SD) inductor by measuring the input capacitance (C_{in}). The effect of using ISD topology for both stages (LNA-1) and first stage only (LNA-2) on the overall NF has been analyzed in detail. It is shown that LNA-1 having ISD HEMTs at both stages demonstrates better NF than LNA-2 having ISD HEMT at the first stage while CS HEMT at the second stage. In this work, role of the stabilization techniques in improving the performance parameters has been demonstrated for the first time. Resistive stability networks lead to maximum available gain (MAG) drop and minimum noise figure (NF_{min}) increase. Stability networks are designed in such a way to minimize this effect for in-band frequencies. Moreover, the S-probe utility of PathWave Advanced Design System (ADS) from Keysight Technologies, Inc. (Santa Rosa, CA 95403, USA) is used to ensure the stability of the device after the complete design.

To the best of the authors' knowledge, for LNA-1, NF less than 1.2 dB is the best reported for X-band GaN-based designs to date. Moreover, this NF value is better than most state-of-the-art X-band LNAs reported using GaAs, SiGe BiCMOS, and CMOS technologies as compared in Table 1. This study is a valuable contribution toward the efforts where GaN LNAs NF becomes even better than GaAs LNAs in X-band.

1099047x, 2022, 11, Downloaded from https://onlinelibrary.wiley.com/doi/10.1002/mmce.23379 by Bilkent University, Wiley Online Library on [22/02/2023]. See the Terms and Conditions (https://onlinelibrary.wiley.com/terms-and-conditions) on Wiley Online Library for rules of use; OA articles are governed by the applicable Creative Commons License

1099047x, 2022, 11, Downloaded from https://onlinelibrary.wiley.com/doi/10.1002/mmce.23379 by Bilkent University, Wiley Online Library on [22/02/2023]. See the Terms and Conditions (https://onlinelibrary.wiley.com/terms-and-conditions) on Wiley Online Library for rules of use; OA articles are governed by the applicable Creative Commons License

Another novel aspect of the article is demonstrating the simultaneous matching of power and gain for ISD HEMTs to achieve a higher output power at 1-dB compression point (P_{1dB}) and third-order intercept point (OIP3). In this context, power and gain load-pull contours have been shown in Section 2.1, while LNA's P_{1dB} and OIP3 results are discussed in Section 3.

2 | LNA MMICS DESIGN

2.1 | HEMTs′ characterization and selection

Active and passive devices are fabricated using NANOTAM's 0.15 μm GaN-on-SiC technology. The device and MMIC's fabrication process is discussed in detail in the authors' earlier works.[34,35,36] Small-signal and noise characterization for HEMTs and MMICs are performed using PNA-X from Keysight Technologies, Inc. (Santa Rosa, CA 95403, USA), ZVA40 from Rohde & Schwarz (München, Germany), and RF and DC probes from GGB industries Inc. (Naples, FL 34104, USA). AMCAD Engineering's (Limoges 87 068, France) IVCAD software, Maury's (Maury Microwave Technologies, Ontario, CA 91764, USA) tuners, and FormFactor's (FormFactor Inc., Livermore, CA 94551, USA) probe station are additionally used for large-signal characterization.

Two HEMTs have been characterized for the proposed LNAs design, both 4 × 75 μm periphery, one with CS and the other with ISD topology. The layouts of both HEMTs are shown in Figure 1. From the small-signal

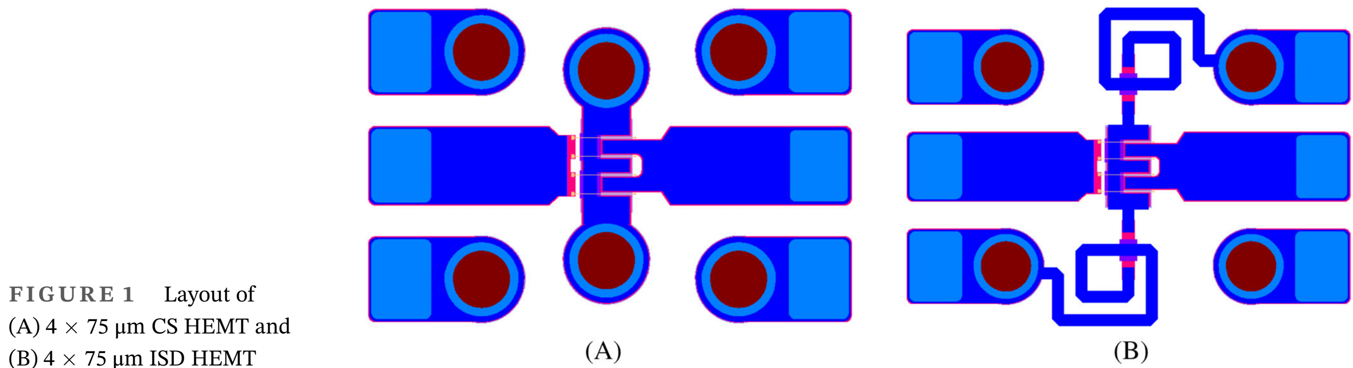

FIGURE 1 Layout of (A) 4 × 75 μm CS HEMT and (B) 4 × 75 μm ISD HEMT

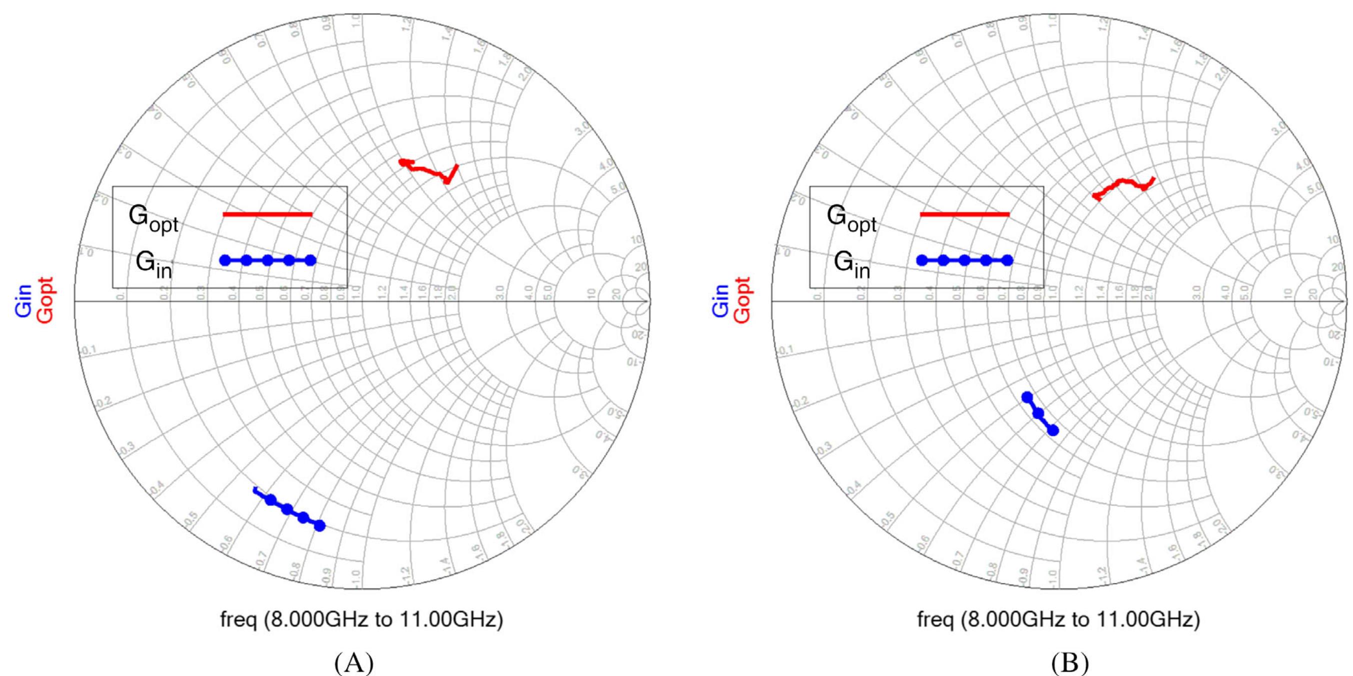

FIGURE 2 Γ_{opt} and Γ_{in} of (A) 4 × 75 μm CS HEMT and (B) 4 × 75 μm ISD HEMT

measurements of the CS HEMT, C_{in} is measured as 0.3 pF in X-band. Therefore, an SD inductor of 0.75 nH is designed and modeled in ADS to resonate with C_{in}, moving the input impedance closer to the resistive part of the smith chart.

Figure 2 shows input impedance (Γ_{in}) and optimum noise impedance (Γ_{opt}), denoted by G_{in} and G_{opt}. An advantage of using ISD HEMTs for designing low noise amplifiers is that Γ_{in} becomes the conjugate of Γ_{opt}, as evident from Figure 2. It allows the designer to match NF and input reflection coefficient (IRC) simultaneously. Another advantage of using ISD topology is the stabilization of HEMT with a minimum increase in NF, which is the main parameter of an LNA design. The stability in the high-frequency range is achieved with the help of a stability resistor at the output drain bias line, while the lower frequency band stabilization is done with the help of gate and drain bias line bypass capacitors. On the other hand, CS HEMTs are not easy to stabilize without introducing a resistive network at the input, which leads to increased NF. This is the main reason for choosing ISD HEMTs, particularly at the first stage in the presented designs. This design aspect will be discussed in further detail in Section 2.2.

Figure 3 shows the MAG and NF_{min} curves for CS and ISD HEMTs. The gain for CS is more than ISD

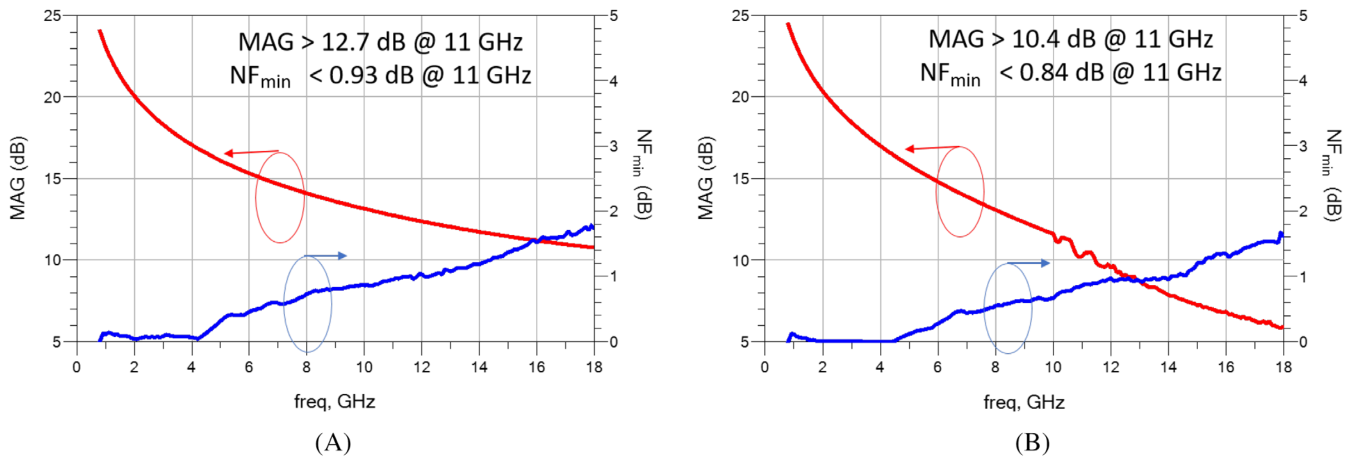

FIGURE 3 MAG and NF_{min} of (A) 4 × 75 μm CS HEMT and (B) 4 × 75 μm ISD HEMT for 12 V, 200 mA/mm

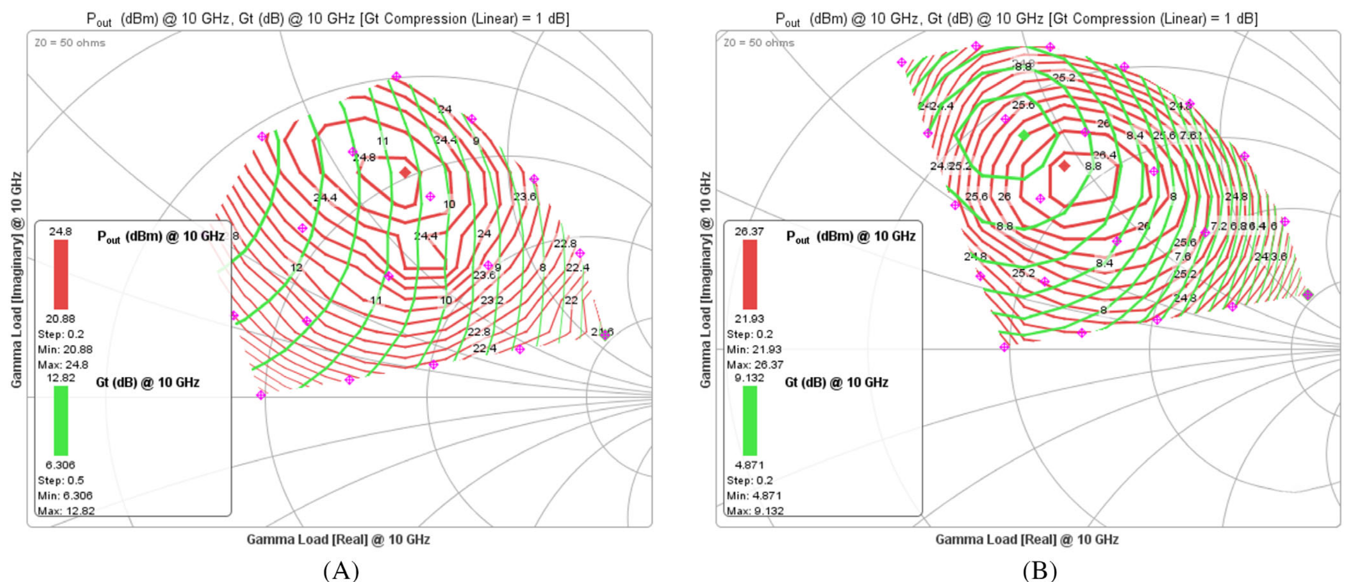

FIGURE 4 Load pull contours for (A) 4 × 75 μm CS HEMT and (B) 4 × 75 μm ISD HEMTs at 10 GHz for 12 V, 200 mA/mm

1099047x, 2022, 11, Downloaded from https://onlinelibrary.wiley.com/doi/10.1002/mmce.23379 by Bilkent University, Wiley Online Library on [22/02/2023]. See the Terms and Conditions (https://onlinelibrary.wiley.com/terms-and-conditions) on Wiley Online Library for rules of use; OA articles are governed by the applicable Creative Commons License

topology, while there is a slight variation in NF_{min}. Figure 4 shows the large-signal characterization where the load circles and gain circles for maximum output are close to each other in the case of ISD HEMT. This gives another advantage of simultaneously matching the output for maximum gain and power performance. This way, an improved P_{1dB} value and a better output reflection coefficient (ORC) are achieved. Higher P_{1dB} leads to better output OIP3, leading to improved linearity of the LNA. Despite the lower gain, ISD HEMT is an obvious choice to achieve a low NF in an LNA design due to abovementioned advantages. The reduction of NF in a multistage LNA design will be discussed in Section 2.2.

2.2 | MMICs design

Two 2-stage LNA MMICs are designed, namely LNA-1 and LNA-2. LNA-1 has 4 × 75 μm ISD HEMTs at both stages, while LNA-2 has the same HEMT at the first stage while 4 × 75 μm CS HEMT at the second stage. The contribution of each stage towards NF in both designs and its impact on overall NF is explored. Figure 5A,B shows

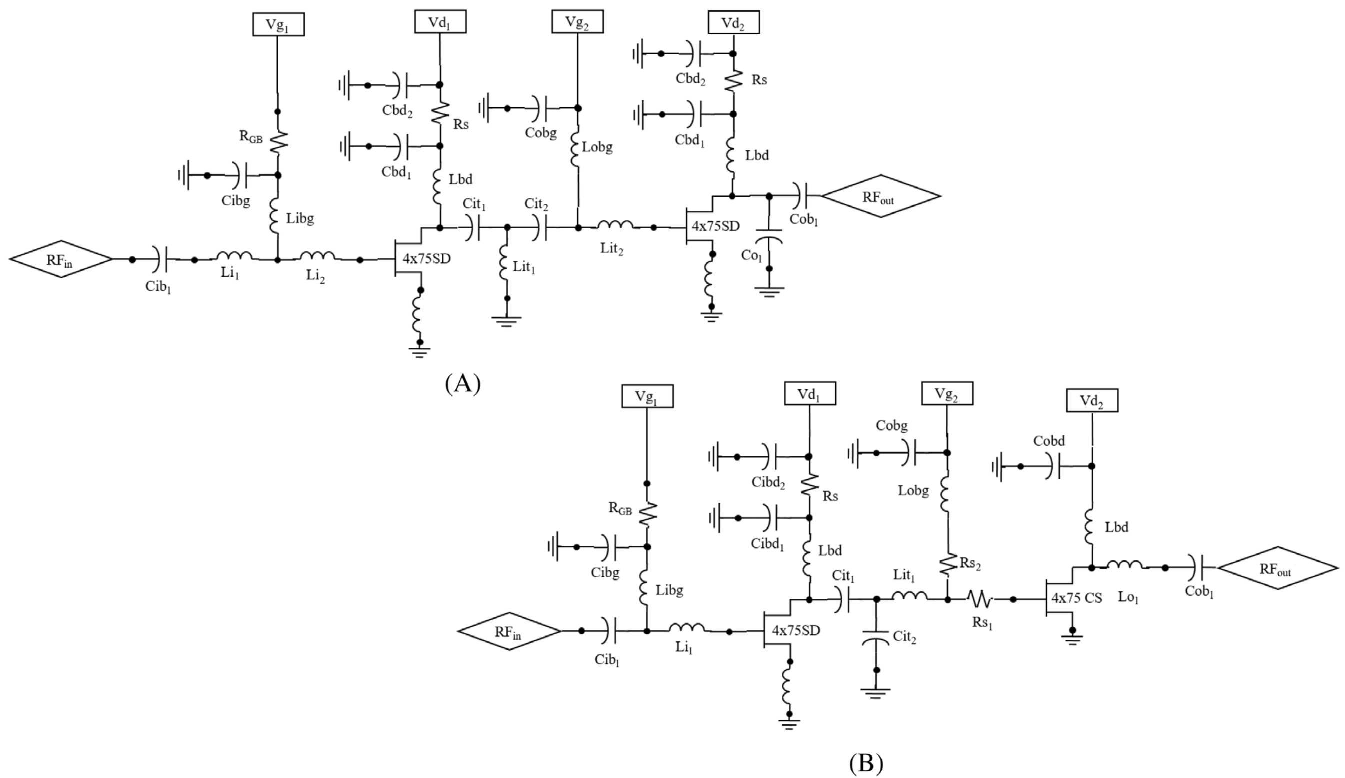

FIGURE 5 Schematic diagram of (A) LNA-1 having ISD HEMTs at both stages (B) LNA-2 having ISD HEMT at the first stage and CS HEMT at the second stage

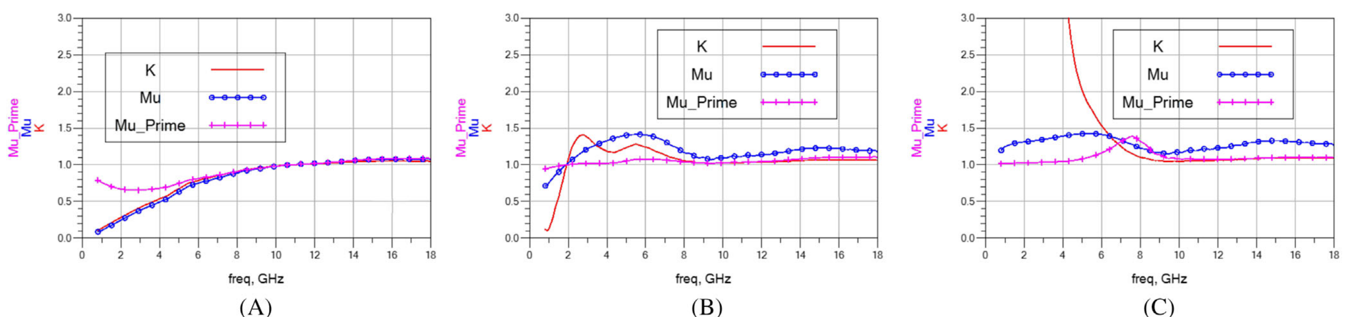

FIGURE 6 Stability parameters of the ISD HEMT (A) without any stabilization network (B) with stability network at the drain side (C) with overall input and output stability networks

1099047x, 2022, 11, Downloaded from https://onlinelibrary.wiley.com/doi/10.1002/mmce.23379 by Bilkent University, Wiley Online Library on [22/02/2023]. See the Terms and Conditions (https://onlinelibrary.wiley.com/terms-and-conditions) on Wiley Online Library for rules of use; OA articles are governed by the applicable Creative Commons License

schematic diagrams of the proposed LNA-1 and LNA-2, respectively.

2.2.1 | HEMTs stabiltity, NF_{min}, and MAG

The stability of the HEMT is determined by three parameters, namely stability (K) factor, μ, and μ'. The stability parameters of the ISD-HEMT are shown in Figure 6A. For the frequencies greater than 2 GHz, ISD-HEMT at the first stage is stabilized using the network containing *Lbd*, *Rs*, *Cbd1*, and *Cbd2* (Figure 5A) toward the drain side, as shown in Figure 6B. Further stability for the lower frequencies is achieved using *Li2*, *Libg*, and *Cibg*. Figure 6C shows that the condition for unconditional stability is fulfilled for lower frequencies. The increase in NF_{min} after stabilization is only 0.16 dB, while MAG is dropped by 0.8 dB only, as evident from Figure 7. A similar procedure is adopted to stabilize the HEMT used for the second stage of LNA-1. R_{GB} is a high value (1 kΩ in this design) first-stage gate bias resistor used to enhance the survivability and does not affect the RF performance.[37] The significance of the R_{GB} in terms of survivability is discussed in one of the authors' earlier works.[34]

Figure 8A shows the stability parameters of CS HEMT without any stabilization network. Referring to Figure 5B, CS HEMT at the second stage is stabilized using a resistive network, Rs_1, and Rs_2, toward the gate side, along with bias capacitors and part of the matching networks containing *Logb*, *Cobg*, *Lbd*, *Cobd*, and *Lo1*. Figure 8B shows the fulfillment of the condition for unconditional stability. NF_{min} is increased to 4.2 dB at 8 GHz, while MAG is dropped to 11.6 dB, as shown in Figure 9. The increase in NF_{min} in the case of CS HEMT is more than ISD-HEMT due to the resistive stability network towards the gate side. This is one of the reasons to use ISD-HEMT at the first stage for both

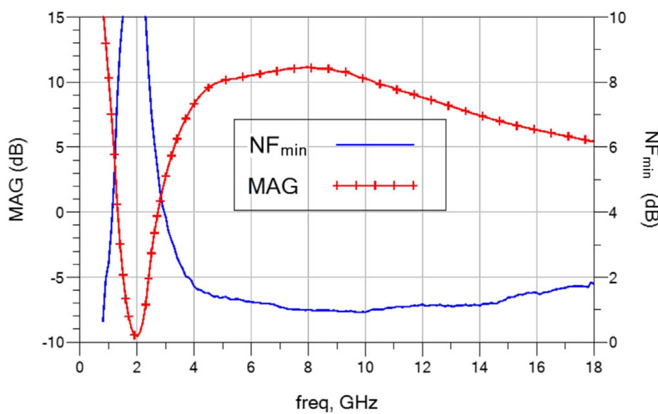

FIGURE 7 NF_{min} and MAG after stabilization of ISD HEMT

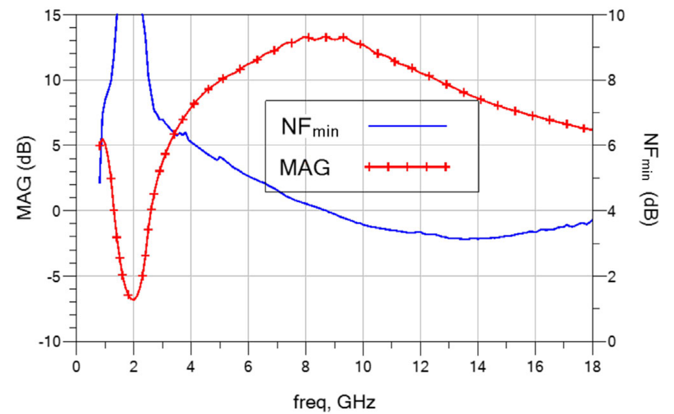

FIGURE 9 NF_{min} and MAG after stabilization of CS HEMT

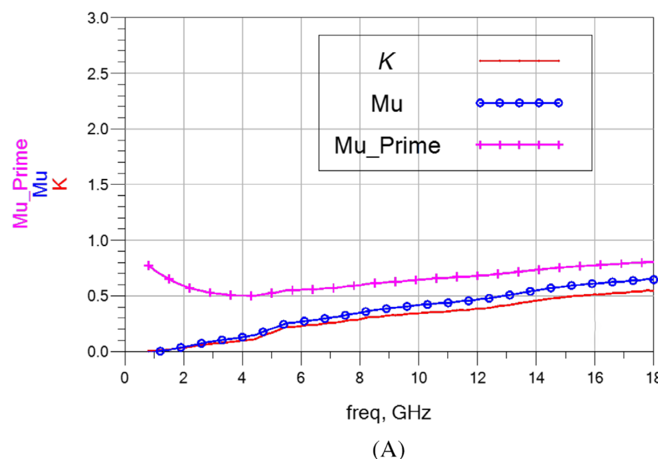

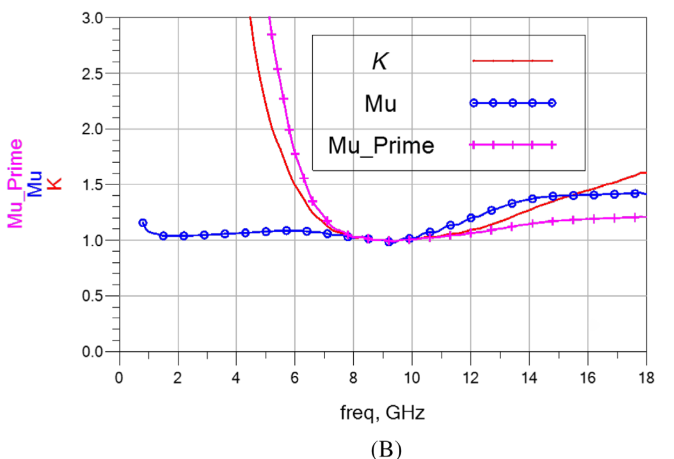

FIGURE 8 Stability parameters of the CS HEMT (A) without any stabilization network (B) with overall input and output stability networks

1099047x, 2022, 11, Downloaded from https://onlinelibrary.wiley.com/doi/10.1002/mmce.23379 by Bilkent University, Wiley Online Library on [22/02/2023]. See the Terms and Conditions (https://onlinelibrary.wiley.com/terms-and-conditions) on Wiley Online Library for rules of use; OA articles are governed by the applicable Creative Commons License

LNA-1 and LNA-2. Although the contribution in overall NF due to the second stage is less, as evident from (1), it still contributes around 0.3 dB to the overall NF for LNA-2.

$$F = F_1 + \frac{F_2 - 1}{G_1} \tag{1}$$

Here F is the NF of the overall system, while F_1 and G_1 are NF and gain of the first stage, respectively, while F_2 is the NF of the second stage.

Figures 6C and 8B show that the K, μ, and μ' stability parameters are close to 1. In order to ensure that there are no even-mode oscillations after completion of the whole design, another technique of the S-probe tool in ADS is used for both LNA-1 and LNA-2. This analysis is discussed in detail in Section 2.2.3.

A slight increase in NF_{min} after stabilization is an indication of a good choice of ISD-HEMT for the first stage, in particular for both designs.

2.2.2 | MMICs' simulation results

After achieving unconditional stability, matching networks are completed at the input, output, and inter-stage. The stability networks discussed in Section 2.2.1 are additionally serving the purpose of matching as well as gate and drain bias. This leads to a compact and efficient design. For LNA-1 and LNA-2, the components other than stability networks in Figure 5 complete the input, output, and inter-stage matching networks.

Electromagnetic (EM) simulations are performed using ADS. Simulations for LNA-1 result in an over-

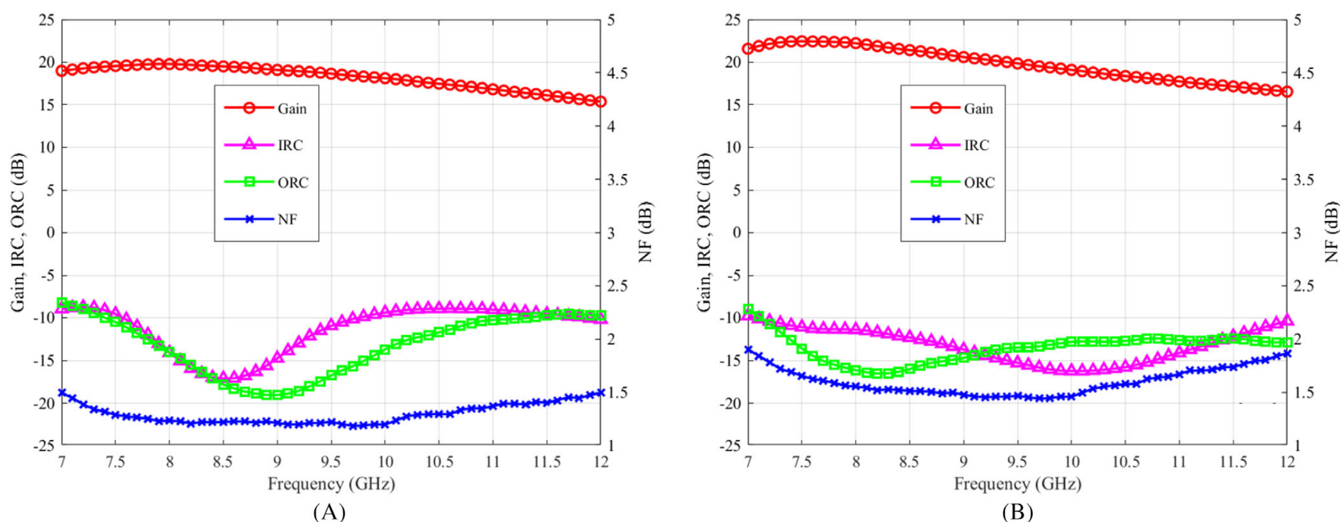

FIGURE 10 Small-signal simulated gain, IRC, ORC, and NF of (A) LNA-1 (B) LNA-2

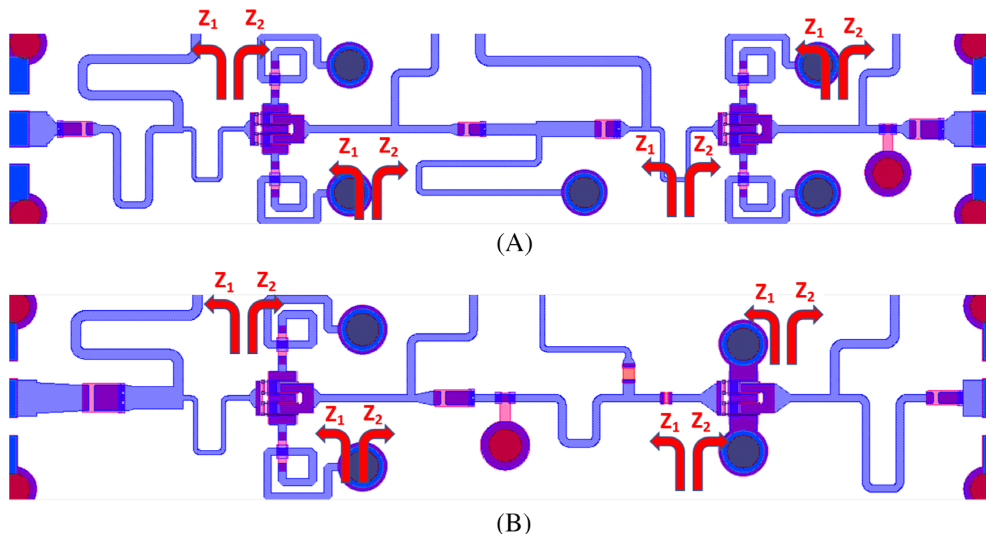

FIGURE 11 The impedances seen at the gate and drain side of the HEMTs using S-probe for (A) LNA-1 (B) LNA-2

1099047x, 2022, 11, Downloaded from https://onlinelibrary.wiley.com/doi/10.1002/mmce.23379 by Bilkent University, Wiley Online Library on [22/02/2023]. See the Terms and Conditions (https://onlinelibrary.wiley.com/terms-and-conditions) on Wiley Online Library for rules of use; OA articles are governed by the applicable Creative Commons License

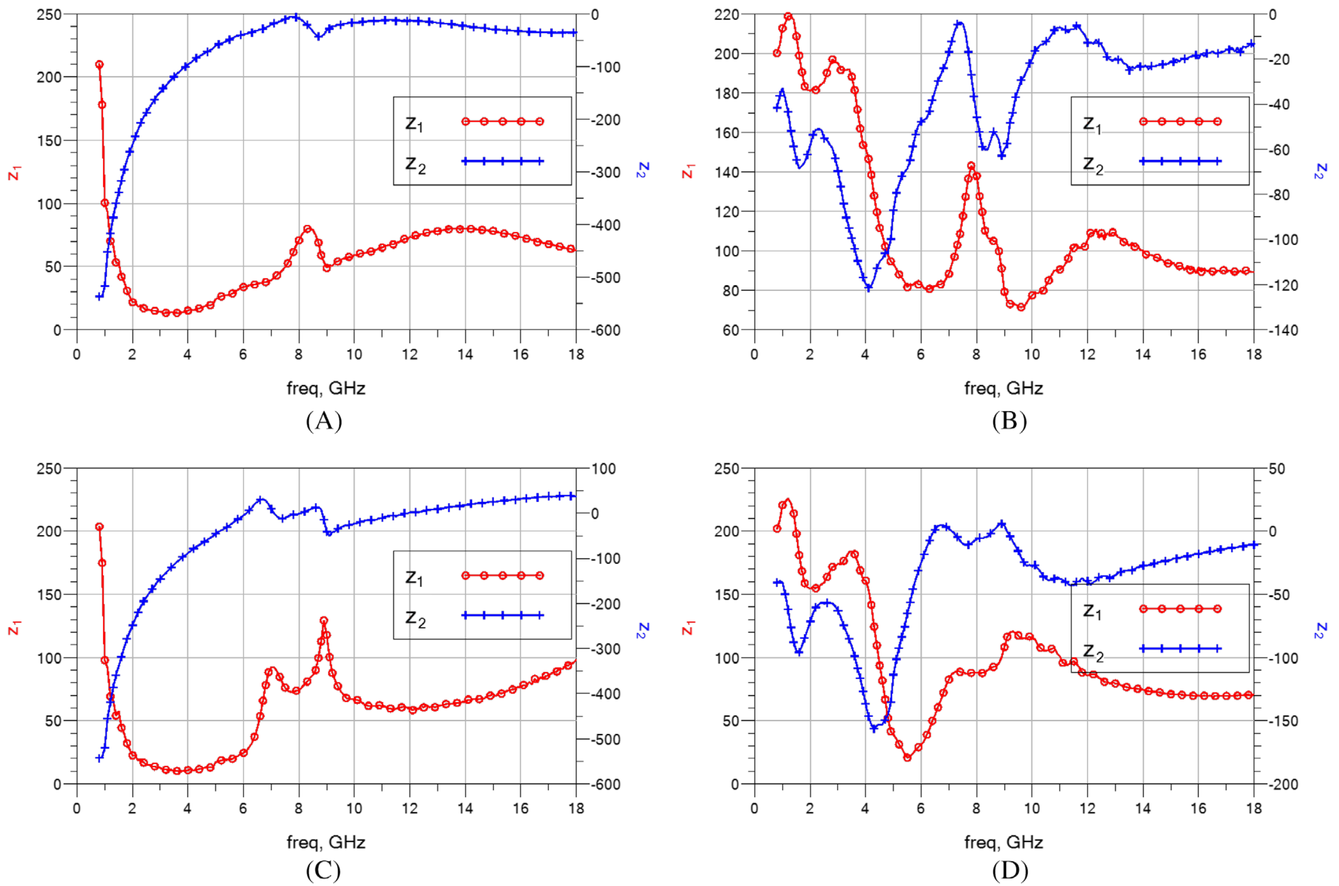

FIGURE 12 LNA-1 even-mode oscillations conditions check at (A) the gate of the first stage HEMT (B) drain of the first stage HEMT (C) gate of the second stage HEMT and (D) drain of the second stage HEMT

all IRC < −8.9 dB, ORC < −10.2 dB, NF < 1.4, and gain > 16.8 dB from 8 to 11 GHz, as evident from Figure 10A. For LNA-2, as shown in Figure 10B, simulated IRC < −11.4 dB, ORC < −12.6 dB, NF < 1.7, and gain > 17.7 dB are achieved in the desired frequency band. To achieve these results, it is important to mention that all the matching networks must be tuned and optimized simultaneously. The reason is that the matching networks affect each other due to smaller HEMTs peripheries and thus having little reverse isolation.

2.2.3 | MMICs' stabiltity consideration

The even-mode stability analysis of the complete layout of the MMIC is performed using the S-probe tool of ADS. Condition for any even-mode oscillation is checked by calculating the impedances toward and away from the gate and drain side of the HEMTs at both stages, as shown in Figure 11.

The condition for oscillations is defined by the following set of equations[38,39,40]:

$$z_1 = \mathrm{Re}((Z_1 + Z_2), f) < 0 \tag{2}$$

$$z_2 = \mathrm{Im}((Z_1 + Z_2), f) = 0 \tag{3}$$

$$\partial z_2 / \partial f > 0 \tag{4}$$

where Z_1 and Z_2 are impedances seen towards and away from the gate and drain side of the HEMTs. In order for the oscillations to occur, the conditions in (2), (3), and (4) should simultaneously be satisfied at a particular frequency. For the oscillations to occur, if z_1 is negative at a particular frequency, there must be a zero-crossing for z_2 with a positive slope. Figures 12 and 13 show that z_1 is always positive all gates and drains of the designed LNAs. Hence, the condition for even-mode oscillation is not satisfied for any of the stages in LNA-1 and LNA-2, ensuring the stability of the devices. As discussed in Section 2.2.1, the stability parameters were kept close to 1 during the design process to have a minimum decrease in MAG and a minimum increase in NF_{min}. Therefore, the S-probe analysis gives the designers an added advantage in solving any oscillation issue before fabrication.

1099047x, 2022, 11, Downloaded from https://onlinelibrary.wiley.com/doi/10.1002/mmce.23379 by Bilkent University, Wiley Online Library on [22/02/2023]. See the Terms and Conditions (https://onlinelibrary.wiley.com/terms-and-conditions) on Wiley Online Library for rules of use; OA articles are governed by the applicable Creative Commons License

3 | FABRICATION RESULTS AND DISCUSSIONS

A microphotograph of the fabricated MMIC is shown in Figure 14. Figure 15A and B show the small-signal and noise measurement results of fabricated LNA-1 and LNA-2 MMICs, respectively. LNA-1 results in gain > 16.8 dB, IRC < −10.3 dB, ORC < −10.1 dB, and NF < 1.2 dB, while for LNA-2, NF < 1.7 dB, IRC < −11.6 dB, ORC < −9.2 dB, and gain > 17.2 dB is achieved. Transistors at both stages for LNA-1 after stabilization have only 1 dB NF_{min}, resulting in an overall NF of 1.2 dB, the best-reported X-band design with two or more stages to the best of the authors' knowledge. For LNA-2, as discussed in Section 2.2, NF_{min} for the second stage CS HEMT after stabilization is 4.2 dB, thus increasing the overall NF to 1.7 dB. One advantage of

FIGURE 13 LNA-2 even-mode oscillations conditions check at (A) the gate of the first stage HEMT (B) drain of the first stage HEMT (C) gate of the second stage HEMT and (D) drain of the second stage HEMT

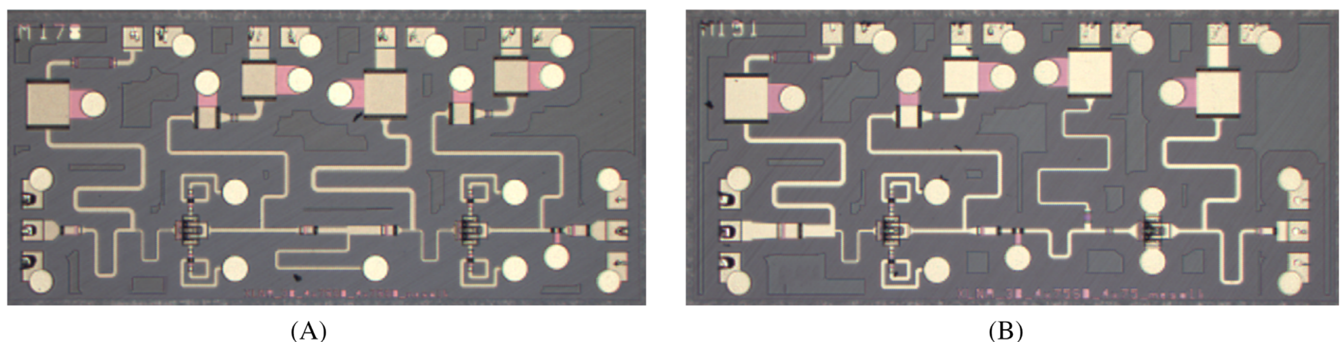

(A) (B)

FIGURE 14 Microphotograph of (A) LNA-1 having ISD HEMTs at both stages (B) LNA-2 having ISD HEMT at the first stage and CS HEMT at the second stage

1099047x, 2022, 11, Downloaded from https://onlinelibrary.wiley.com/doi/10.1002/mmce.23379 by Bilkent University, Wiley Online Library on [22/02/2023]. See the Terms and Conditions (https://onlinelibrary.wiley.com/terms-and-conditions) on Wiley Online Library for rules of use; OA articles are governed by the applicable Creative Commons License

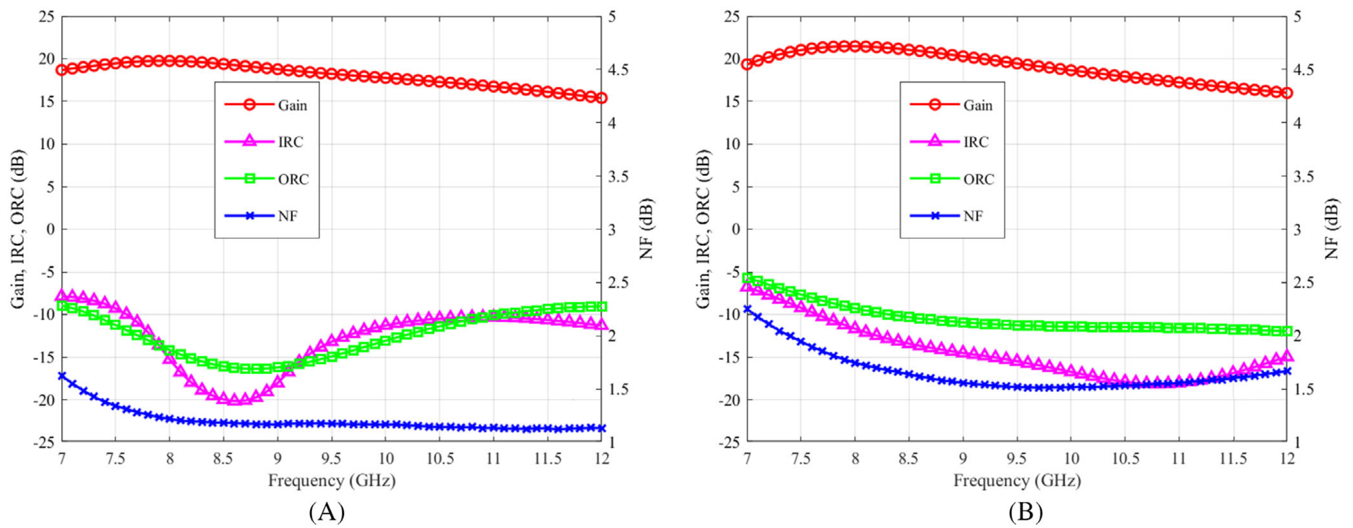

FIGURE 15 Measured gain, IRC, ORC, and NF of (A) LNA-1 (B) LNA-2

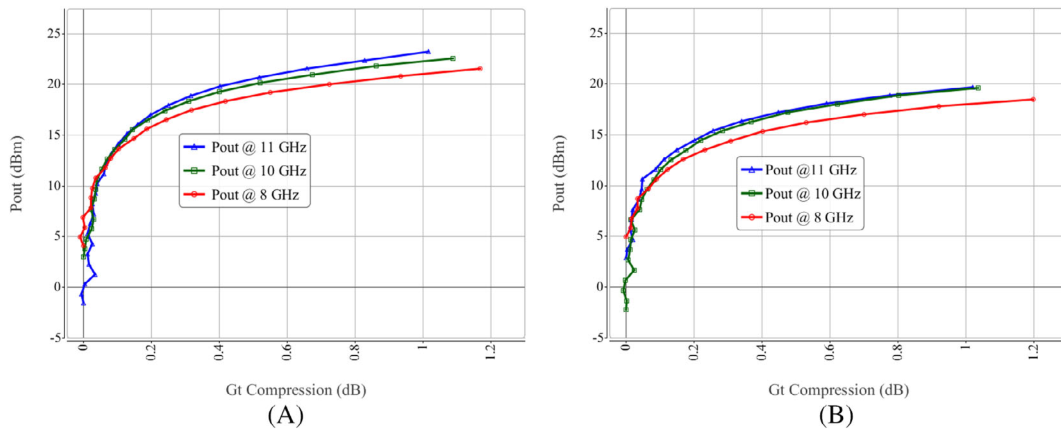

FIGURE 16 P_{1dB} of fabricated (A) LNA-1 (B) LNA-2 at 8 GHz, 10 GHz, and 11 GHz for 12 V 200 mA/mm

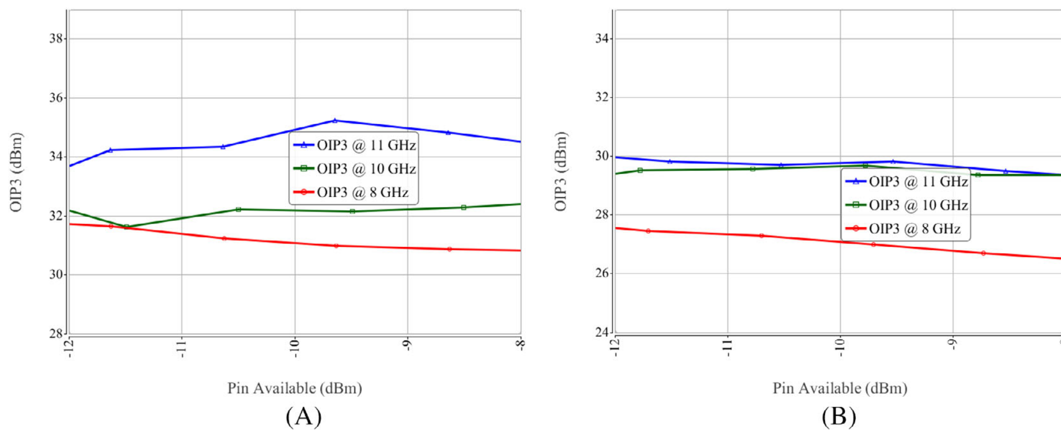

FIGURE 17 OIP3 of fabricated (A) LNA-1 (B) LNA-2 at 8 GHz, 10 GHz, and 11 GHz for 12 V 200 mA/mm

1099047x, 2022, 11, Downloaded from https://onlinelibrary.wiley.com/doi/10.1002/mmce.23379 by Bilkent University, Wiley Online Library on [22/02/2023]. See the Terms and Conditions (https://onlinelibrary.wiley.com/terms-and-conditions) on Wiley Online Library for rules of use; OA articles are governed by the applicable Creative Commons License

TABLE 2 A comparison of designed MMIC with the recent GaN-based works at X-band

Ref.	Freq. (GHz)	NF (dB)	Gain (dB)	IRC (dB)	ORC (dB)	P_{1dB} (dBm)	OIP3 (dBm)	Lg (μm)
Micovic et al.[41]	4–16	<2.0	>11	<−10	<−8	–	24	0.15
Kobayashi et al.[42]	9–11	<2.2	>13.5	<−11	<−5	–	29.5–34.5	0.15
Zafar et al.[34]	8–11	<2.0	>19	<−9	<−11	>19	30.5–34.2	0.15
Colangeli et al.[43]	8.4–10.6	<2.3	>25	<−10[b]	<−12[b]	–	–	0.25
Kazan et al.[44]	8–11	<2.0	>22	<−9	<−5	–	24–29	0.25
Kim and Ga o[45]	8–11	<2.2	>25	<−8[b]	<−10[b]	16	26	0.25
Janssen et al.[46]	8–11[b]	<2.3	>16	–	–	–	–	0.25
Bettidi et al.[47]	8–11	<2.5	>17	<−10[b]	<−8.5[b]	>17	–	–
Andrei et al.[48]	7–12	<2.5	>14	<−5[b]	<−5[b]	20	28	0.25
Chang et al.[49]	9.7–12.9	<2.1	>20	<−2[b]	<−7[b]	–	32	0.25
Helali et al.[50a]	8–12	<2.4	>20	<−4	<−3	–	–	–
Vittori et al. (LNA A)[51]	8–10	<1.3	>24	<−2	<−4	21[b]	33.8	0.25
Vittori et al. (LNA B)[51]	10–12	<1.75	>24.4	<−10	<−12.5	20[b]	32.8	0.25
Angelo et al.[52]	7.4–11.4	<1.6	>23	<−10	<−10	23	–	0.25
Schuh and Reber[53]	8–12	<1.8	>14	–	–	–	19.5	0.25
Yağbasan and Aktuğ[21]	8–11	<1.6	>22.5	<−10	<−8	12	24	0.25
Kobayashi et al.[22]	9–11	<1.5	>13.5	<−10	<−8[b]	–	33–36	0.09
This work (LNA-1)	8–11	<1.2	>16.8	<−10.3	<−10.1	>21	31–34	0.15
This work (LNA-2)	8–11	<1.7	>17.2	<−11.6	<−9.2	>17	27–30	0.15

[a]Simulation based.
[b]Estimated values from the figures.

using CS HEMT in LNA-2 is higher gain than LNA-1 but at the cost of higher NF. To conclude, the choice of ISD-HEMT in subsequent stages of a multistage LNA design is desirable to achieve low NF values. Gain compensation may be achieved by increasing the number of stages, although at the cost of the size.

P_{1dB} for LNA-1 and LNA-2 is shown in Figures 16 and 17, respectively. A noticable difference of higher P_{1dB} for LNA-1 with ISD HEMT is evident compared to LNA-2 with CS HEMT at the second stage. Similar results for OIP3 measurements are achieved with LNA-1 having a higher OIP3 value, as shown in Figure 17. Table 2 shows the comparative analysis of this work with recently published X-band LNAs. Both LNA-1 and LNA-2 have promising values of NF, gain, IRC, ORC, P_{1dB}, and OIP3. LNA-1 has the best reported NF in X-band compared with published designs using 0.25, 0.15, and 0.09 μm technologies.

4 | CONCLUSION

This article demonstrates two GaN-based X-band LNAs using 0.15 μm technology. ISD HEMTs, easy to stabilize and maintain a low NF_{min} after stabilization, are proven to be an optimum choice for all the stages in a multi-stage design to achieve overall low NF. Moreover, through simultaneous match conditions for ISD topology, minimum noise and a low IRC are achieved at the same time. Before fabrication, S-probe analysis is performed in ADS to check for any even-mode oscillation. LNA-1 achieves sub-1.2 dB NF and IRC better than −10.3 dB due to optimized stability networks and matching techniques. Small signal gain > 16.8 dB, ORC < −10.1 dB, P_{1dB} > 21 dBm, and OIP3 > 31 dBm for LNA-1 are achieved. LNA-2 having ISD HEMT at the first stage and common source (CS) at the second stage obtains NF < 1.7 dB and IRC < −11.6 dB. Moreover, gain > 17.2 dB, ORC < −9.2 dB, P_{1dB} > 21 dBm, and OIP3 > 27 dBm for LNA-2 are obtained. Sub-1.2 dB NF of LNA-1 is best for GaN-based X-band LNAs reported to date to the best of the authors' knowledge. This NF value is comparable with other competitive GaAs and SiGe technologies known for best noise performance.

ACKNOWLEDGMENTS

The authors are obliged to NANOTAM's fabrication and measurement teams in general, and Emirhan Urfalı, Efkan Güneysu, Mahmut Can Soydan, Armağan Gürdal, and Yilmaz Durna in particular. Ekmel Ozbay also acknowledges the partial support from the Turkish Academy of Sciences.

1099047x, 2022, 11, Downloaded from https://onlinelibrary.wiley.com/doi/10.1002/mmce.23379 by Bilkent University, Wiley Online Library on [22/02/2023]. See the Terms and Conditions (https://onlinelibrary.wiley.com/terms-and-conditions) on Wiley Online Library for rules of use; OA articles are governed by the applicable Creative Commons License

CONFLICT OF INTEREST

The authors declare no potential conflict of interests.

DATA AVAILABILITY STATEMENT

Research data are not shared.

ORCID

Salahuddin Zafar https://orcid.org/0000-0002-5212-9602

REFERENCES

1. Yoon HS, Min BG, Lee JM, et al. Microwave low-noise performance of 0.17 μm gate-length AlGaN/GaN HEMTs on SiC with wide head double-deck T-shaped gate. *IEEE Electron Device Lett*. 2016;37(11):1407-1410. doi:10.1109/LED.2016.2612624
2. Rudolph M. GaN HEMTs for low-noise amplification—status and challenges. Paper presented at: 2017 Integrated Nonlinear Microwave and Millimetre-wave Circuits Workshop (INMMiC), 2017: 1–4. 10.1109/INMMIC.2017.7927327
3. Tong X, Zhang S, Xu J, et al. 18-31 GHz GaN wideband low noise amplifier (LNA) using a 0.1 μm T-gate high electron mobility transistor (HEMT) process. *Int J RF Microw Comput-Aid Eng*. 2018;28(8):e21425. doi:10.1002/mmce.21425
4. Zheng P, Zhang S, Xu J, Wang R, Tong X. A 23–31 GHz robust low-noise amplifier with 1.1 dB noise figure and 28 dBm Psat. Paper presented at: 2019 49th European Microwave Conference (EuMC) 2019: 801–803. 10.23919/EuMC.2019.8910749.
5. Pace L, Colangeli S, Ciccognani W, et al. Design and validation of 100 nm GaN-on-Si Ka-band LNA based on custom noise and small signal models. *Electronics*. 2020;9(1):1-14. doi:10.3390/electronics9010150
6. R V, Gorre P, Song H, Kumar S. Highly robust X-band quasi circulator-integrated low-noise amplifier for high survivability of radio frequency front-end systems. *Int J Circuit Theory Appl*. 2021;49(7):2170-2182. doi:10.1002/cta.3001
7. Çalışkan C, Kalyoncu I, Yazıcı M, Kaynak M, Gurbuz Y. Ultra-low noise amplifier for X-band SiGe BiCMOS phased Array applications. *IEEE Trans Circuits Syst II Express Briefs*. 2019;66(9):1507-1511. doi:10.1109/TCSII.2019.2891133
8. Davulcu M, Çalışkan C, Kalyoncu l, Gurbuz Y. An X-band SiGe BiCMOS triple-Cascode LNA with boosted gain and P_{1dB}. *IEEE Trans Circuits Syst II Express Briefs*. 2018;65(8):994-998. doi:10.1109/TCSII.2018.2800284
9. Kanar T, Rebeiz GM. X- and K-band SiGe HBT LNAs with 1.2- and 2.2-dB mean noise figures. *IEEE Trans Microwave Theory Techn*. 2014;62(10):2381-2389. doi:10.1109/TMTT.2014.2341218
10. Ciccognani W, Colangeli S, Serino A, et al. Comparative noise investigation of high-performance GaAs and GaN millimeter-wave monolithic technologies. Paper presented at: 2019 14th European Microwave Integrated Circuits Conference (EuMIC). 2019: 192–195. 10.23919/EuMIC.2019.8909484.
11. Colangeli S, Vittori M, Ciccognani W, Limiti E. Three-stage GaN-on-SiC medium-power LNA exploiting a current-reuse architecture. *Int J RF Microwave Comput-Aid Eng*. 2018;28(9):e21423. doi:10.1002/mmce.21423
12. Cao C, Li Y, Wang Z, et al. CMOS X-band pole-converging triple-cascode LNA with low-noise and wideband performance. *IET Circuits Devices Sys*. 2021;16(1):26-39. doi:10.1049/cds2.12081
13. Zailer E, Belostotski L, Plume R. Wideband LNA noise matching. *IEEE Solid-State Circuits Lett*. 2020;3:62-65. doi:10.1109/LSSC.2020.2986645
14. Sabzi M, Kamarei M, Haghighi TR, Mahe Y. Analysis and design of X-band LNA using parallel technique. Paper presented at: 2020 28th Iranian Conference on Electrical Engineering (ICEE). 2020: 1–5. 10.1109/ICEE50131.2020.9260604
15. Dai R. A 0.6-V sub-mW X-band RFSOI CMOS LNA with novel complementary current-reused technique. *Int J Circuit Theory Appl*. 2017;45(12):2046-2056. doi:10.1002/cta.2336
16. Sabzi M, Kamarei M, Razban T, Mahe Y. Optimization of LNA's first stage to reduce overall noise figure in multi-stage LNAs. *AEU-Int J Electron C*. 2020;123:153300. doi:10.1016/j.aeue.2020.153300
17. Zou Y, Chen Z, Lai J, Li B, Wu Z, Lin X. Design of Ka-band broadband low-noise amplifier using 100nm gate-length GaN on silicon technology. *J Phys Conf Ser*. 2021;1983:012080. doi:10.1088/1742-6596/1983/1/012080
18. Zhang S, Xu J, Zheng P, Wang R, Tong X. An 18–31-GHz GaN-based LNA with 0.8-dB minimum NF and high robustness. *IEEE Microwave Wireless Compon Lett*. 2020;30(9):896-899. doi:10.1109/LMWC.2020.3011135
19. Tong X, Zhang S, Zheng P, et al. A 22–30-GHz GaN low-noise amplifier with 0.4–1.1-dB noise figure. *IEEE Microwave Wireless Compon Lett*. 2019;29(2):134-136. doi:10.1109/LMWC.2018.2886074
20. Salvucci A, Longhi PE, Colangeli S, Ciccognani W, Serino A, Limiti E. A straightforward design technique for narrowband multi-stage low-noise amplifiers with I/O conjugate match. *Int J RF Microwave Comput-Aid Eng*. 2019;29(9):e21833. doi:10.1002/mmce.21833
21. Yağbasan C, Aktuğ A. Robust X-band GaN LNA with integrated active limiter. Paper presented at: 2018 48th European Microwave Conference (EuMC). 2018: 1205–1208. 10.23919/EuMC.2018.8541779.
22. Kobayashi KW, Kumar V, Campbell C, Chen S, Cao Y, Jimenez J. Robust-5W reconfigurable S/X-band GaN LNA using a 90nm T-gate GaN HEMT technology. Paper presented at: 2020 IEEE BiCMOS and Compound Semiconductor Integrated Circuits and Technology Symposium (BCICTS). 2020: 1–4. 10.1109/BCICTS48439.2020.9392933
23. Sabzi M, Medi A. Analysis and design of multi-stage wideband LNA using simultaneously noise and impedance matching method. *Microelectr J*. 2019;86:97-104. doi:10.1016/j.mejo.2019.03.004
24. Feng C, Yu XP, Lu ZH, Lim WM, Sui WQ. 3–10 GHz self-biased resistive-feedback LNA with inductive source degeneration. *Electr Lett*. 2013;49(6):387-388. doi:10.1049/el.2012.4472
25. Ciccognani W, Limiti E, Longhi PE, Renvoise M. MMIC LNAs for Radioastronomy applications using advanced industrial 70 nm metamorphic technology. *IEEE J Solid-State Circuits*. 2010;45(10):2008-2015. doi:10.1109/JSSC.2010.2058170
26. Nguyen TK, Kim CH, Ihm GJ, Yang MS, Lee SG. CMOS low-noise amplifier design optimization techniques. *IEEE Trans Microwave Theory Techn*. 2004;52(5):1433-1442. doi:10.1109/TMTT.2004.827014
27. Shaeffer D, Lee T. A 1.5-V, 1.5-GHz CMOS low noise amplifier. *IEEE J Solid-State Circuits*. 1997;32(5):745-759. doi:10.1109/4.568846

1099047x, 2022, 11, Downloaded from https://onlinelibrary.wiley.com/doi/10.1002/mmce.23379 by Bilkent University, Wiley Online Library on [22/02/2023]. See the Terms and Conditions (https://onlinelibrary.wiley.com/terms-and-conditions) on Wiley Online Library for rules of use; OA articles are governed by the applicable Creative Commons License

28. Jarndal AH, Bassal AM. A broadband hybrid GaN cascode low noise amplifier for WiMax applications. *Int J RF Microwave Comput-Aid Eng*. 2019;29(10):e21456. doi:10.1002/mmce.21456
29. Zuo Z, Sun S. X-band monolithic three-stage LNA with GaAs E-mode PHEMT. *J Phys Conf Ser*. 2021;1971:012004. doi:10.1088/1742-6596/1971/1/012004
30. Xie C, Yu Z, Tan C. An X/Ku dual-band switch-free reconfigurable GaAs LNA MMIC based on coupled line. *IEEE Access*. 2020;8:160070-160077. doi:10.1109/ACCESS.2020.3020396
31. Wang C, Chen KY, Lee YL, Li CH. A X-/K_u-band QFN-packaged GaAs LNA supporting dual-polarization signal reception. Paper presented at: 2019 IEEE Asia-Pacific Microwave Conference (APMC). 2019: 1521–1523. 10.1109/APMC46564.2019.9038788
32. Zhou X, Li Y, Zhou G, Wei H, Gao X, Wu H. Design of X-band miniature balanced limiter-low noise amplifier chip. Paper presented at: 2018 International Conference on Microwave and Millimeter Wave Technology (ICMMT). 2018: 1–3. 10.1109/ICMMT.2018.8563840
33. Ma C, Wu H, Lu X, Sun H. Research and design of X-band low noise amplifier based on CMOS process. *J Phys Conf Ser*. 2021; 2108:012102. doi:10.1088/1742-6596/2108/1/012102
34. Zafar S, Cankaya Akoglu B, Aras E, et al. Design and robustness improvement of high-performance LNA using 0.15 μm GaN technology for X-band applications. *Int J Circuit Theory Appl*. 2022;50(7):2305-2319. doi:10.1002/cta.3286
35. Zafar S, Osmanoglu S, Ozturk M, et al. GaN based LNA MMICs for X-band applications. Paper presented at: 2020 17th International Bhurban Conference on Applied Sciences and Technology (IBCAST). 2020: 699–702. 10.1109/IBCAST47879.2020.9044569
36. Zafar S, Osmanoglu S, Cankaya B, Kashif A, Ozbay E. GaN-on-SiC LNA for UHF and L-band. Paper presented at: 2019 European Microwave Conference in Central Europe (EuMCE). 2019: 95–98.
37. Rudolph M, Behtash R, Doerner R, et al. Analysis of the survivability of GaN low-noise amplifiers. *IEEE Trans Microwave Theory Techn*. 2007;55(1):37-43. doi:10.1109/TMTT.2006.886907
38. Freitag R. A unified analysis of MMIC power amplifier stability. Paper presented at: 1992 IEEE MTT-S Microwave Symposium Digest. 1992: 297–300, 1. 10.1109/MWSYM.1992.187971
39. Jankowski M, Limiti E, Longhi PE. Freitag method application to PA stability test. Paper presented at: 2008 Workshop on Integrated Nonlinear Microwave and Millimetre-Wave Circuits. 2008: 149–152. 10.1109/INMMIC.2008.4745739
40. Cankaya Akoglu B, Sutbas B, Ozbay E. High efficiency 35 GHz MMICs based on 0.2 μm AlGaN/GaN HEMT technology. *Int J Microwave Wireless Technol*. 2022;n/a(n/a):1-9. doi:10.1017/S1759078722000617
41. Micovic M, Kurdoghlian A, Lee T, et al. Robust broadband (4 GHz - 16 GHz) GaN MMIC LNA. Paper presented at: 2007 IEEE Compound Semiconductor Integrated Circuits Symposium. 2007: 1–4. 10.1109/CSICS07.2007.54
42. Kobayashi KW, Campbell C, Lee C, Gallagher J, Shust J, Botelho A. A reconfigurable S−/X-band GaN cascode LNA MMIC. Paper presented at: 2017 IEEE Compound Semiconductor Integrated Circuit Symposium (CSICS). 2017: 1–4. 10.1109/CSICS.2017.8240424
43. Colangeli S, Bentini A, Ciccognani W, Limiti E, Nanni A. GaN-based robust low-noise amplifiers. *IEEE Trans Electr Devices*. 2013;60(10):3238-3248. doi:10.1109/TED.2013.2265718
44. Kazan O, Kocer F, Aydin Civi O. An X-band robust GaN low-noise amplifier MMIC with sub 2 dB noise figure. Paper presentedat: 2018 13th European Microwave Integrated Circuits Conference (EuMIC). 2018: 234–236. 10.23919/EuMIC.2018.8539909.
45. Kim B, Gao W. X-band robust current-shared GaN low noise amplifier for receiver applications. Paper presented at: 2016 IEEE Compound Semiconductor Integrated Circuit Symposium (CSICS). 2016: 1–4. 10.1109/CSICS.2016.7751081
46. Janssen JPB, Heijningen VM, Provenzano G, Visser GC, Morvan E, Vliet VFE. X-band robust AlGaN/GaN receiver MMICs with over 41 dBm power handling. Paper rpesented at: 2008 IEEE Compound Semiconductor Integrated Circuits Symposium. 2008: 1–4. 10.1109/CSICS.2008.23
47. Bettidi A, Corsaro F, Cetronio A, Nanni A, Peroni M, Romanini P. X-band GaN-HEMT LNA performance versus robustness trade-off. Paper presented at: 2009 European Microwave Conference (EuMC). 2009: 1792–1795. 10.23919/EUMC.2009.5296145.
48. Andrei C, Doerner R, Bengtsson O, Chevtchenko SA, Heinrich W, Rudolph M. Highly linear X-band GaN-based low-noise amplifier. Paper presented at: 2012 International Symposium on Signals, Systems, and Electronics (ISSSE). 2012: 1–4. 10.1109/ISSSE.2012.6374314
49. Chang W, Jeon GI, Park YR, Mun JK. X-band MMIC low-noise amplifier MMIC on SiC substrate using 0.25-μm ALGaN/GaN HEMT technology. *Microw Opt Technol Lett*. 2014;56(1):96-99. doi:10.1002/mop.28044
50. Helali A, Gassoumi M, Gassoumi M, Gassoumi M. Design and optimization of LNA amplifier based on HEMT GaN for X-band wireless-communication and IoT applications. *Silicon*. 2021;13:2645-2653. doi:10.1007/s12633-020-00626-8
51. Vittori M, Colangeli S, Ciccognani W, Salvucci A, Polli G, Limiti E. High performance X-band LNAs using a 0.25 μm GaN technology. Paper presented at: 2017 13th Conference on Ph.D. Research in Microelectronics and Electronics (PRIME). 2017: 157–160. 10.1109/PRIME.2017.7974131
52. D'Angelo S, Biondi A, Scappaviva F, Resca D, Monaco VA. A GaN MMIC chipset suitable for integration in future X-band spaceborne radar T/R module frontends. Paper presented at: 2016 21st International Conference on Microwave, Radar and Wireless Communications (MIKON). 2016: 1–4. 10.1109/MIKON.2016.7492014
53. Schuh P, Reber R. Robust X-band low noise limiting amplifiers. Paper presented at: 2013 IEEE MTT-S International Microwave Symposium Digest (MTT). 2013: 1–4. 10.1109/MWSYM.2013.6697551

How to cite this article: Zafar S, Aras E, Akoglu BC, et al. Design of GaN-based X-band LNAs to achieve sub-1.2 dB noise figure. *Int J RF Microw Comput Aided Eng*. 2022;32(11):e23379. doi:10.1002/mmce.23379

1099047x, 2022, 11, Downloaded from https://onlinelibrary.wiley.com/doi/10.1002/mmce.23379 by Bilkent University, Wiley Online Library on [22/02/2023]. See the Terms and Conditions (https://onlinelibrary.wiley.com/terms-and-conditions) on Wiley Online Library for rules of use; OA articles are governed by the applicable Creative Commons License